

# L-arginine increases UVA cytotoxicity in irradiated human keratinocyte cell line: potential role of nitric oxide

CHRISTINE DIDIER,\* NATHALIE EMONET-PICCARDI,\* JEAN-CLAUDE BÉANI,\* JEAN CADET,<sup>†</sup> AND MARIE-JEANNE RICHARD\*<sup>1</sup>

\*LBSO/LCR7 No. 8-Université Joseph Fourier, F-38043 Grenoble Cedex 03, France; and

<sup>†</sup>Laboratoire Lésions des Acides Nucléiques, Département de Recherche Fondamentale sur la Matière Condensée, Service de Chimie Inorganique et Biologie, CEA/Grenoble, F-38054 Grenoble Cedex 9, France

**ABSTRACT** Human fibroblasts and keratinocytes possess nitric oxide synthases (NOS), which metabolize L-arginine (L-Arg) for producing nitric oxide (NO<sup>•</sup>). This report delineates the relations between NO<sup>•</sup> and UVA in the human keratinocyte cell line HaCaT. NOS activity was stimulated by exposure of cells to L-Arg just after irradiation. L-Arg (5 mM) supply led to an increase in UVA (25.3 J/cm<sup>2</sup>) cytotoxicity (% of viability 18 ± 3%) whereas neither L-Arg itself nor UVA irradiation induced cell death at the doses used in this study. Cells were also treated either with L-thiocitrulline (L-Thio), an irreversible inhibitor of NOS, or with exogenous superoxide dismutase (SOD) and catalase. L-Thio and SOD prevented L-Arg-mediated deleterious effects in irradiated cells, whereas catalase was ineffective. Intracellular antioxidant enzyme activities were also determined. UVA/L-Arg stress altered catalase (66% decrease) and glutathione peroxidase (83% decrease). DNA damage was evaluated using the 'comet assay' and quantified using the 'tail moment'. UVA alone was genotoxic (mean tail moment: 25.43 ± 1.23, *P* < 0.001 compared control cells). The addition of L-Arg potentiated DNA damage (mean tail moment: 41.05 ± 3.9) whereas L-Thio prevented them (mean tail moment 9.86 ± 0.98). We attempted to assess the effect of poly(ADP-ribose) polymerase (PARP) inhibition on cell death. Using the PARP inhibitor 3-aminobenzamide, we established that PARP determines both cell lysis and DNA damage induced by UVA and/or L-Arg. Our findings demonstrated that L-Arg was able to increase UVA-mediated deleterious effects in keratinocytes (both DNA damage and cytotoxicity) and that the ratio NO<sup>•</sup>/O<sub>2</sub><sup>-•</sup> plays a key role in these processes.—Didier, C., Emonet-Piccardi, N., Béani, J.-C., Cadet, J., Richard, M.-J. L-arginine increases UVA cytotoxicity in irradiated human keratinocyte cell line: potential role of nitric oxide. *FASEB J.* 13, 1817–1824 (1999)

*Key Words:* DNA damage • NO • metalloenzymes • SNAP

NITRIC OXIDE (NO<sup>•</sup>),<sup>2</sup> which is secreted from various cell types under both physiological and pathophysiological conditions, contributes to a variety of regulatory biological processes. These include the regulation of vascular tone, the modulation of synaptic transmission in the brain, together with antimicrobial and antitumor activities (1). Nevertheless, NO<sup>•</sup> appears to have both toxic and protective effect (2) and may have a role in the pathogenesis of some diseases such as inflammation (3) and cancer (4).

Recent studies from Baudouin and Tachon (5), Villiotou and Deliconstantinos (6) have shown that normal human keratinocytes constitutively expressed an isoform of nitric oxide synthase (NOS), which is Ca<sup>2+</sup>/calmodulin dependent. More recently, Wang et al. (7) demonstrated that unstimulated human skin fibroblasts expressed only Ca<sup>2+</sup>-dependent/NOS activity whereas cells stimulated with cytokines and lipopolysaccharides expressed both constitutive (Ca<sup>2+</sup>-dependent/NOS) and inducible (Ca<sup>2+</sup> independent/NOS) ones. Although constitutive and inducible NOS isoforms can be expressed in all cell types of human skin (4), the subsequent regulatory and cytotoxic effects of NO<sup>•</sup> in skin are not well known. In the skin, NO<sup>•</sup> could participate to the deleterious effect of ultraviolet (UV) irradiation, in conjugation with others reactive oxygen species (ROS) produced during the photo-

<sup>1</sup> Correspondence: LBSO, Laboratoire de Biochimie C, C. H. U. Albert Michallon, 38043 Grenoble Cedex 03, France. E-mail: Marie-Jeanne Richard @ ujf-grenoble.fr

<sup>2</sup> Abbreviations: ABA, 3-aminobenzamide; CuZn SOD, copper/zinc superoxide dismutase; GSH-Px, glutathione peroxidase; H<sub>2</sub>O<sub>2</sub>, hydrogen peroxide; L-Arg, L-arginine; L-Thio, L-thiocitrulline; MnSOD, manganese superoxide dismutase; NO<sup>•</sup>, nitric oxide; NOS, nitric oxide synthases; O<sub>2</sub><sup>-•</sup>, superoxide anion; ONOO<sup>-</sup>; peroxynitrite; PARP, poly (ADP-ribose) polymerase; PBS, phosphate-buffered saline; ROS, reactive oxygen species; SNAP, S-nitroso-N-acetylpenicillamine; SOD, superoxide dismutase; UVA, ultraviolet radiation (320–400 nm).

oxidation of intracellular components by ultraviolet radiation (UVA-2, 320–340 nm and UVA-1, 340–400 nm). Indeed, the effectiveness of NO<sup>•</sup> as a cytotoxic molecule is modulated by ROS such as the superoxide anion radical (O<sub>2</sub><sup>•-</sup>) and hydrogen peroxide (H<sub>2</sub>O<sub>2</sub>). The interaction of NO<sup>•</sup> with O<sub>2</sub><sup>•-</sup> yields the peroxynitrite anion (ONOO<sup>-</sup>) and increases the reactivity of the two individual molecules toward targets of cellular metabolism (3, 8, 9). In fact, most of the cytotoxic properties of NO<sup>•</sup> have been attributed to the formation of ONOO<sup>-</sup> (10) although nitrite, a major product of NO metabolism, can also readily promote protein nitration via reactions with peroxidases (11). Villiotou and Deliconstantinos (6) showed that UVA-irradiated human squamous cell carcinoma (SCC-13) released reactive nitrogen oxides, as evidenced by increased nitrite/nitrate production and products of protein nitration. Formation and/or release of these reactive nitrogen oxides by UVA were time and concentration dependent. Their levels were significantly decreased by addition of a specific inhibitor of NOS, namely, *N*-monomethyl-L-arginine.

In the present study, we provide evidence that L-arginine (L-Arg), the substrate of NOS, increased the deleterious effects induced by UVA irradiation in the human keratinocyte cell line HaCaT. To elucidate the respective roles of ROS and NO<sup>•</sup> in UVA/L-Arg-mediated cytotoxicity, 1) the production of NO<sup>•</sup> was measured, 2) the alterations of the intracellular antioxidant metalloenzymes were assessed, 3) DNA damage was determined, and 4) the potential role of poly(ADP-ribose) polymerase (PARP) in UVA/L-Arg-treated cells was evaluated.

## MATERIALS AND METHODS

### Materials

RPMI 1640 and fetal calf serum were purchased from ATGC (ATGC Biotechnologie, Noisy-le-Grand, France). L-glutamine was obtained from Boehringer (Mannheim, Germany), whereas penicillin and streptomycin were from Polylabo (Paul Block, Strasbourg, France). Phosphate-buffered saline (PBS) without calcium and magnesium was purchased from Eurobio (Les Ulis, France). *S*-Nitroso-*N*-acetyl D,L penicillamine (SNAP), L-Arg, catalase (from bovine liver, 21,000 units/mg protein), superoxide dismutase (from bovine erythrocytes; 4400 units/mg protein), and other reagents were purchased from Sigma Chemical Co. (St. Louis, Mo.). L-thiocitrulline (L-Thio) was obtained from Calbiochem (La Jolla, Calif.).

### Cell culture

Keratinocytes immortalized from a spontaneously transformed human epithelial cell line (HaCaT) were kindly supplied to us by Dr. Fusenig (12). They were routinely cultured at 37°C in a humidified atmosphere (5% CO<sub>2</sub> in air) in RPMI 1640 containing 1 mM L-Arg, supplemented with

10% fetal calf serum, 3.6 mM L-glutamine, 4.5 U·ml<sup>-1</sup> penicillin, and 0.045 U·ml<sup>-1</sup> streptomycin. For each study, cells were plated onto 9 cm<sup>2</sup> petri dishes from Life Technologies, Inc. (Grand Island, N.Y.) and grown for 4 days to near confluency. The culture medium was replaced by fresh medium 48 h before the experiment.

### UVA irradiation

The UVA source was a high-pressure Tecimex apparatus (Verre & Quartz-Dixwell, Bondy, France). The emission maximum of the lamp was centered at 372 nm. The UVA doses effectively received from the bottom by the cells were evaluated with a radiometer (Verre & Quartz). Prior to irradiation, the culture medium was removed and reserved. Cells were rinsed twice with 1.5 ml of PBS and left in 1 ml of PBS. Control cells were similarly treated but left in the dark instead to be irradiated. Three UVA doses were applied: 25.3, 50.5, and 67.3 J·cm<sup>-2</sup>.

### NO<sup>•</sup> sources

Two different NO<sup>•</sup>-generating systems were used. SNAP (0.02 M) was dissolved in PBS just before use and diluted in the medium to a final concentration of 750 μM. The solution of L-Arg, the specific substrate of NOS, was also prepared just before use and applied on near-confluent cells to final concentrations varying from 0.5 to 10 mM. To study the interaction between UVA radiation and L-Arg, the amino acid was added to the culture medium immediately after the irradiation and the cells were then reincubated for 18 h.

### Other treatments

To assess the ability of metalloenzymes to prevent UVA/L-Arg induced damage catalase (500 U/ml) and/or SOD (0.44 U/ml) were added immediately after the irradiation.

The stock solution of 0.1 M L-Thio, an irreversible inhibitor of NOS, was prepared in ethanol, diluted first in deionized water and then added to the culture medium (100, 250 μM) just before L-Arg treatment.

Cells were treated with 3-aminobenzamide (ABA, 1 mM) just after irradiation in order to study the link between DNA damage, cell death, and activation of the nuclear PARP.

### Assay of cell viability

Cell viability was evaluated using the neutral red technique. After irradiation and/or chemical treatment, cells were incubated for 18 h in their reserved medium. A solution of neutral red (50 mg/l) was made with the cell culture medium and 3 ml was added to the dishes. Then cells were reincubated for 3 h at 37°C, resulting in the uptake of the vital dye into viable cells. The dye medium was removed and the cells were washed rapidly with 4% formaldehyde-1% CaCl<sub>2</sub> to remove extraneously adhering, unincorporated dye, according to Borenfreund and Puerner (13). Neutral red was extracted into 3 ml of a mixture of 1% acetic acid-50% ethanol. After 20 min, the absorbances were measured with a spectrophotometer set at 540 nm. The results represent the means of three experiments with two petri dishes for each condition (Cc, control cells; Tlc, treated irradiated cells). The results were expressed as the viability (%) evaluated from the formula (Tlc/Cc) \* 100.

## Alkaline single-cell gel electrophoresis

The procedure already described (14) was modified as follows. Typically, 150  $\mu\text{l}$  of 0.6% normal melting agarose in PBS was dropped onto frosted microscope slides (Touzart et Matignon, Les Ullis, France), covered with a coverslip, and kept at room temperature until subsequent use. Cells in petri dishes were treated (irradiation or/and application of L-Arg). Three hours later, HaCaT cells were trypsinized and the cell pellet was suspended in PBS. About 20,000 cells were mixed with 75  $\mu\text{l}$  of 0.6% low melting point agarose (FMC Bioproducts, Rockland, Maine) in PBS. The slides were kept in the dark at 4°C in order to limit nonspecific DNA damage and repair process. A final layer of agarose (75  $\mu\text{l}$  of 0.6% low melting point agarose) was applied. Each slide was processed in duplicate, as described previously (15), and examined using an epifluorescence microscope, Zeiss Axioskop 20 (Carl Zeiss, Microscope Division, Oberkochen, Germany), equipped with a mercury lamp HBO (50 W, 516–560 nm, Zeiss) and filters 5 and 15 (Zeiss) at  $\times 20$  magnification. Fifty randomly selected comets on each duplicated slide were scored with a pulmix TM 765 camera (Kinetic Imaging, Liverpool, U.K.), linked to a Komet 3.0 image analysis system (Kinetic Imaging, U.K.). The software allows measurement of the fluorescence intensity of the head and tail regions along with determination of their length. The quantification of DNA damage was performed using the tail moment, the product of the tail distance, and the percent of DNA in the tail (relative to the amount of DNA in the entire comet).

## Metalloenzymes activities

Keratinocytes in 75  $\text{cm}^2$  culture flasks (NUNC, Grand Island, N.Y.) were incubated in the presence of either 750  $\mu\text{M}$  SNAP or 5 mM L-Arg for 18 h. After two washings with PBS, the cells were harvested and frozen-defrozen five times. The homogenates were centrifuged for 10 min at 4000 rpm at 4°C. The supernatants were stored at  $-80^\circ\text{C}$  until metalloenzymes analysis. The glutathione peroxidase (GSH-Px) activity was determined as described previously (16), using tert-butyl hydroperoxide as the substrate. This was achieved by following the decrease in NADPH concentration at 340 nm. Catalase activity was determined by the method of Beers and Sizer (17) by following the decomposition of  $\text{H}_2\text{O}_2$  at 240 nm. Manganese (MnSOD) and copper/zinc (CuZn SOD) superoxide dismutase activities were determined as described previously (18) by monitoring the rate of the oxidation of pyrogallol by superoxide radicals. The specific inhibition of CuZn SOD by 9 mM potassium thiocyanate allows MnSOD determination by the same procedure. Each sample was assayed twice and results were expressed as SOD units (1 U is the amount of SOD inhibiting the reaction rate by 50% in the given assay conditions). Enzymatic activities were normalized to the soluble cell protein content determined by the Micro BCA protein assay (Pierce, Rockford, Ill.). The results of five replicate experiments are given.

## Statistical analysis

All data, expressed as mean  $\pm$  standard deviation, were processed statistically using the Student's *t* test. Differences were considered to be significant when  $P < 0.05$ .

## RESULTS

### Enhancement of UVA cytotoxicity by L-Arg

Figure 1 illustrates the promoting effect of L-Arg,

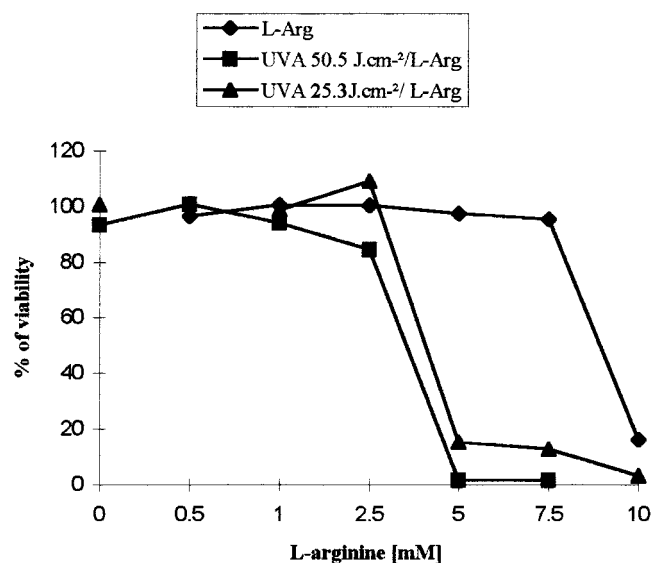


**Figure 1.** Cell viability in UVA/L-Arg-treated cells. HaCat cells were irradiated (25.3 J/cm<sup>2</sup>, 50.5 J/cm<sup>2</sup>) or sham irradiated. L-Arg at different concentrations (0–10 mM) was added to the culture medium just after irradiation, as described in Material and Methods. The percentage survival was calculated using the formulas (ICc/Cc) \* 100 and (Tic/Tc) \* 100. ICc, irradiated control cells; Cc, control cells; Tic, treated irradiated cells; Tc, treated cells. The results are presented as mean  $\pm$  standard deviation ( $n=3$ ).

added at different concentrations to the culture medium, on the UVA cytotoxicity. Cell viability was not modified significantly by the irradiation at the fluences used ( $100.7 \pm 1.5\%$ ,  $93.4 \pm 2.1\%$  for 25.3 and 50.5 J/cm<sup>2</sup>, respectively). Low concentrations of L-Arg were found to have no effect on cell viability. Treatment with L-Arg (5 mM and 7.5 mM) immediately after UVA irradiation led to a significant decrease in cell viability ( $P < 0.001$ ) compared with irradiation alone. These results demonstrate that L-Arg potentiates the lethal effect of UVA and suggest that NOS are stimulated.

### NOS involvement in the lethal effects of UVA/L-Arg treatment

Under basal conditions, the release of  $\text{NO}^\bullet$  by HaCaT keratinocytes over 24 h is very low. This was illustrated by the fact that the level of nitrites in the culture medium was below the detection threshold of the Greiss reaction ( $< 3 \text{ nmol}/10^6 \text{ cells}/18 \text{ h}$ ). However, the amount of  $\text{NO}^\bullet$  released by cells exposed to UVA/L-Arg (25.3 J/cm<sup>2</sup>/5 mM) treatment increased more than sixfold ( $20 \pm 5 \text{ nmol}/10^6 \text{ cells}/18 \text{ h}$ ). To assess the involvement of  $\text{NO}^\bullet$  or  $\text{ONOO}^-$  in the cytotoxic effect of UVA/L-Arg treatment, we used L-Thio, a stereospecific inhibitor ( $K_i=100 \mu\text{M}$ ) of the constitutive brain and endothelial NOS isoforms. L-Thio is recognized by the active site of NOS and acts with the heme-containing



TABLE 1. Influence of L-thiocitrulline (L-Thio) on the viability of cells exposed to UVA irradiation, L-Arg treatment, or both<sup>a</sup>

	Cc	L-Arg	L-Thio		L-Arg + L-Thio	
			100 μM	250 μM	100 μM	250 μM
-UVA % survival	100	97.5 ± 2.1	106.5 ± 3.0	115.1 ± 18.6	97.1 ± 13.4	85.3 ± 1.8
+UVA % survival	100.7 ± 1.5	15.2 ± 7.3*	103.2 ± 10.5	92.6 ± 2.7	32.9 ± 6.6***	43.5 ± 6.7**

<sup>a</sup> Cells were irradiated (25.3 J/cm<sup>2</sup>) and treated with L-Arg (5 mM) and/or L-Thio (100 and 250 μM). We determined the percentage survival by neutral red technique, as explained in Material and Methods. The results are presented as mean ± standard deviation (*n* = 3). \*\*\**P* < 0.05 and \*\**P* < 0.01, L-Arg+L-Thio vs. L-Arg; \**P* < 0.001, UVA/L-Arg vs. L-Arg.

enzyme, thus giving rise to an irreversible inhibition. From the data listed in **Table 1**, it is clear that the addition of either 100 or 250 μM L-Thio protected keratinocytes (*P* < 0.05 and *P* < 0.01, respectively) against cell death induced by the sequential treatment UVA/L-Arg (25.3 J·cm<sup>-2</sup>/5 mM). These results are in accordance with the levels of nitrite (< 3 nmol/10<sup>6</sup> cells/18 h); L-Thio 250 μM) released in the medium by UVA/L-Arg-treated cells. The protection increased with the concentration of L-Thio, suggesting that NOS are implicated in the observed cytotoxicity.

#### UVA/L-Arg as SNAP treatment altered antioxidants systems

To further study the effect of L-Arg (5 mM) on HaCaT keratinocytes, the intracellular antioxidant metalloenzymes activities were determined 18 h after treatments. **Table 2** summarizes the results. GSH-Px was strongly inhibited when cells were either exposed to UVA radiation (77% decrease relative to control) or cultured in the presence of L-Arg (58% decrease). The inhibition was amplified by the combined treatment UVA/L-Arg (83% decrease). The level of catalase was also significantly affected by UVA, L-Arg, and both sequential treatments (36, 59, and 66% decrease, respectively, relative to control cells). In contrast, the total activity of SOD was not significantly modified. However, an induction of MnSOD was observed in UVA-irradiated cells (45% increase relative to control).

NO<sup>•</sup> has been shown to alter the activities of several enzymes in which thiol groups, heme or nonheme iron, are essential for the catalytic function (19, 20, 21). Thus, the activities of metalloenzymes were determined 18 h after treating the HaCaT cells with 750 μM SNAP (**Table 3**). A significant increase in MnSOD was observed (32% relative to control). Catalase was significantly disturbed and the GSH-Px activity was highly inhibited after the SNAP treatment (respectively 25.5 and 92% decrease relative to control).

#### Modulation of UVA/L-Arg injury by antioxidant metalloenzymes

To determine the nature of reactive species implicated in the UVA/L-Arg cytotoxicity, the assay was conducted in the presence of metalloenzymes (SOD and/or catalase). The results reported in **Table 4** showed that SOD protected the keratinocytes (73% protection compared to treated cells without any antioxidant) whereas catalase was ineffective. However, SOD amplified the deleterious effects of irradiation alone or those of the L-Arg treatment compared to treated cells without any antioxidant. Cell viability decreased by 25 and 48%, respectively.

#### The role of NO<sup>•</sup> and PARP in the DNA damage induced by UVA/L-Arg

To better understand UVA/L-Arg toxicity, DNA damage was determined. Nuclear DNA in nonirradi-

TABLE 2. Modulation of antioxidants metalloenzymes activities by UVA irradiation, L-Arg treatment, or both<sup>a</sup>

	Cc	L-Arg	UVA	UVA/L-Arg
SOD <sub>T</sub> <sup>b</sup>	6.1 ± 0.4	6.2 ± 0.6	7.3 ± 0.9	7.2 ± 1.5
SOD <sub>Mn</sub> <sup>b</sup>	3.1 ± 0.2	3.3 ± 0.8	4.5 ± 0.7*	3.8 ± 0.1
SOD <sub>CuZn</sub> <sup>b</sup>	3.0 ± 0.3	2.9 ± 0.6	2.7 ± 1.6	3.5 ± 1.5
Catalase <sup>b</sup>	21.6 ± 0.4	13.9 ± 1.2**	8.7 ± 1.8***	7.3 ± 3.1 <sup>##</sup>
GSH-Px <sup>b</sup>	174 ± 6.2	72 ± 16.5**	38.5 ± 2.7***	29.4 ± 0.8 <sup>##SS</sup>

<sup>a</sup> SOD, GSH-Px, and catalase activities were determined 18 h after treatments. The results are presented as mean ± standard deviation (*n* = 3). \*\*\**P* < 0.05 UVA vs. control cells (Cc), \*\**P* < 0.01 L-Arg vs. Cc, \**P* < 0.001 UVA vs. Cc. <sup>##</sup>*P* < 0.05 UVA/L-Arg vs. L-Arg, <sup>##</sup>*P* < 0.01 UVA/L-Arg vs. L-Arg, <sup>SS</sup>*P* < 0.01 UVA/L-Arg vs. UVA.

<sup>b</sup> U/mg protein.

TABLE 3. Alteration of enzyme activities in HaCat cells exposed to SNAP<sup>a</sup>

	Cc	SNAP 750 $\mu$ M
	<i>U/mg protein</i>	
SOD <sub>T</sub>	6.1 $\pm$ 0.4	6.9 $\pm$ 0.4***
SOD <sub>Mn</sub>	3.1 $\pm$ 0.2	4.1 $\pm$ 0.7***
SOD <sub>CuZn</sub>	3.0 $\pm$ 0.3	2.8 $\pm$ 0.5
Catalase	21.6 $\pm$ 0.4	16.1 $\pm$ 3.3***
GSH-Px	174 $\pm$ 6.2	13.8 $\pm$ 3.6*

<sup>a</sup>Intracellular activities of SOD, GSH-Px, and catalase were measured after cell incubation in presence or absence of 750  $\mu$ M SNAP for 18 h. Mean  $\pm$  standard deviation of triplicate experiments are indicated. \*\*\* $P$  < 0.05 and \* $P$  < 0.001 SNAP 750  $\mu$ M vs. control cells (Cc).

ated cells was not altered and the tail moment was very low (6.45  $\pm$  0.78), showing that the experimental procedure was tolerated well by the cells (Table 5). The tail moment was not significantly modified in cells treated with 5 mM L-Arg alone. In contrast, even under conditions where UVA did not induce cell death, the tail moment was fourfold greater in UVA-irradiated cells (25.43  $\pm$  1.23,  $P$  < 0.001) than in control cells. The combined sequential treatment involving UVA irradiation (25.3 J/cm<sup>2</sup>) and L-Arg (5 mM) strongly increased the number of alkali-labile sites and DNA strand breaks (41.05  $\pm$  3.9). In cells previously treated by 250  $\mu$ M L-Thio, the mean tail moment (9.86  $\pm$  0.98) was similar to those determined in control cells. These results suggest that L-Arg via the NOS pathway and ROS generated by UVA radiation could interact in inducing DNA fragmentation and cell death. To determine whether PARP activation participates in the observed DNA damage, cells were treated with a PARP inhibitor. ABA (1 mM) was found to enhance the cell viability up to 56.63  $\pm$  5.75% ( $P$  < 0.001 vs. L-Arg/UVA-treated cells without ABA). In addition, ABA had a statistically significant ( $P$  < 0.001) protective effect on UVA/L-Arg-induced DNA damage (Fig. 2). We observed that ABA also prevented DNA damage in UVA-irradiated or L-Arg-treated cells, but this ability was low compared with those observed in UVA/L-Arg cells. These results support the notion that poly-(ADP-ribose)-ation is the primary injury in UVA/L-Arg-treated cells whereas other mechanisms started off in either UVA or L-Arg-treated cells.

TABLE 4. Influence of antioxidant metalloenzymes on the viability of HaCaT cells subjected to UVA irradiation, L-Arg treatment, or both<sup>a</sup>

	Cc	L-Arg	UVA	UVA/L-Arg
Without metalloenzymes	100	97.5 $\pm$ 2.1	100.7 $\pm$ 1.5	15.2 $\pm$ 7.3*
+SOD	110.2 $\pm$ 2.2	50.7 $\pm$ 4.9***	75.7 $\pm$ 7.1***	57.3 $\pm$ 1.9*
+Catalase	97.6 $\pm$ 4.1	86.4 $\pm$ 1.6	113.9 $\pm$ 1.3	12.7 $\pm$ 3.2

<sup>a</sup> Confluent cell monolayers were incubated with SOD (0.44 U/ml) or catalase (500 U/ml) before UVA (25.3 J/cm<sup>2</sup>) or/and L-Arg (5 mM) treatment. Values are represented as mean  $\pm$  standard deviation ( $n$  = 3). \*\*\* $P$  < 0.05 L-Arg+SOD vs. L-Arg and UVA+SOD vs. UVA; \* $P$  < 0.001 UVA/L-Arg+SOD vs. UVA/L-Arg and UVA/L-Arg vs. L-Arg.

## DISCUSSION

The mechanism of sunlight-induced skin damage is one of the most urgent problems to be solved in the field of skin photobiology. Here we studied L-Arg/NO<sup>•</sup> pathway in keratinocytes and investigated the combined effects of UVA radiation and L-Arg on cell cytotoxicity and DNA damage with respect to the levels of NO<sup>•</sup>. Using inhibitors of NOS as well as antioxidant metalloenzymes, it was shown that NO<sup>•</sup> and O<sub>2</sub><sup>-•</sup> are involved in UVA/L-Arg induced injury.

L-Arg, was found to enhance the cytotoxic effect of UVA on cultured the human keratinocyte HaCaT cell line. This essential amino acid is nontoxic at concentrations lower than 7.5 mM, although it is involved in the L-Arg/NO<sup>•</sup> pathway. In contrast, supply of UVA-irradiated cells with L-Arg increased dramatically the UVA cytotoxicity. Recent studies have shown that UVA-irradiated human squamous cell carcinoma (SCC-13) led to the release of the reactive nitrogen species (NO<sub>x</sub>, ONOO<sup>-</sup>). Formation and/or release of these reactive nitrogen species was time- and concentration-dependently stimulated by UVA whereas their level was decreased by N-monomethyl-L-arginine (6). Here it was demonstrated that the release of NO<sup>•</sup> increased significantly in UVA/L-Arg-treated cells (20  $\pm$  5 nmol/10<sup>6</sup> cells/18 h). It should be remembered that HaCaT cells released very weak amounts of NO<sup>•</sup> in the culture medium (<3 nmol/10<sup>6</sup> cells/18 h). These observations are consistent with previous reports on human dermal fibroblasts (7) and human squamous cell carcinoma (6). Moreover, we demonstrated that the NO<sup>•</sup> release was abolished in cells pretreated with L-Thio, a stereospecific inhibitor of NOS, which also largely prevented the UVA/L-Arg cytotoxicity. These results confirm the involvement of NOS in the latter deleterious effect.

Reactive nitrogen species may induce DNA fragmentation (22). Using the comet assay, it was demonstrated that DNA strand breaks and alkali-labile sites induced by the combined treatment UVA/L-Arg increased twofold compared to UVA irradiation alone. When NOS was inhibited by L-Thio, the tail moment decreased significantly both in L-Arg and UVA/L-Arg-treated cells, whereas in UVA-irradiated cells the inhibition of NOS led to a significant

TABLE 5. Effect of L-thiocitrulline (250  $\mu$ M) on DNA damage induced by UVA (25.3 J/cm<sup>2</sup>) and/or L-Arg (5 mM) in HaCaT keratinocytes<sup>a</sup>

	-UVA		+UVA	
	Cc	L-Arg	Cc	L-Arg
Tail moment -L-Thio	6.45 $\pm$ 0.78	10.63 $\pm$ 3.03	25.43 $\pm$ 1.23*	41.05 $\pm$ 3.90**
Tail moment +L-Thio (250 $\mu$ M)	5.66 $\pm$ 0.33	3.86 $\pm$ 0.52*	48.24 $\pm$ 4.25	9.86 $\pm$ 0.98

<sup>a</sup>Yield of damage is represented by the mean tail moment of 50 cells per slide (two slides per conditions and three different experiments). \* $P < 0.001$  UVA vs. control cells (Cc), \*\* $P < 0.01$  L-Arg+UVA vs. L-Arg.

increase in tail moment. These paradoxical results may be related to the balance between reactive nitrogen and reactive oxygen species. The production of NO<sup>•</sup> is not always associated with cellular toxicity (23). Indeed, whereas NO<sup>•</sup> protects against ischemia reperfusion, peroxide-induced toxicity (24, 25), lipid peroxidation (26), and myocardial injury, it can combine with O<sub>2</sub><sup>•-</sup> to form ONOO<sup>-</sup>, which may be protonated to yield peroxynitrous acid. Depending on the pH of the local environment, peroxynitrous acid degrades to either inactive metabolites or toxic radicals. Thus, it appears that NO<sup>•</sup> may behave either as a potentially toxic molecule or as an oxygen free radical scavenger (20). In UVA/L-Arg-treated cells, the simultaneous production of NO<sup>•</sup> and ROS might be led to ONOO<sup>-</sup> formation and the increase in DNA damage might be related to this highly cytotoxic species. Ischiropoulos et al. (9) have reported that inhibition of NO<sup>•</sup> synthesis by N-methyl-L-arginine increases the level of H<sub>2</sub>O<sub>2</sub> arising from the dismutation of superoxide radical in murine macrophages. Thus, we may hypothesize that under conditions where NOS are inhibited by L-Thio, UVA-irradiated HaCaT cells produced essentially ROS (O<sub>2</sub><sup>•-</sup>, H<sub>2</sub>O<sub>2</sub>, and <sup>•</sup>OH). Indeed, L-Thio significantly reduced the tail moment measured in UVA/L-Arg-treated cells, suggesting that the modulation of the flux ratio of ROS relative to NO<sup>•</sup> interfere with the otherwise damaging potency of UVA. Although ONOO<sup>-</sup> might be formed under basal condition and L-Arg treatment, its low production rate does not automatically contribute to the initiation of cell death.

When SOD was added into the medium, L-Arg became cytotoxic whereas catalase had no effect. We postulated that SOD increases the rate of superoxide dismutation into H<sub>2</sub>O<sub>2</sub>, leading to a modification of the ratio between ROS and NO<sup>•</sup>. Under this condition, the low level of superoxide did not allow the generation of ONOO<sup>-</sup>. These results are in accordance with Filep et al. (22), who reported a cooperative effect between nitric oxide and H<sub>2</sub>O<sub>2</sub> in inducing both cell lysis and DNA fragmentation in murine lymphoma cells. Nevertheless, exogenously added SOD conferred protection to UVA/L-Arg-treated cells, whereas catalase did not. The final outcome of the biological reactions of NO<sup>•</sup> is likely to be deter-

mined by the rate of NO<sup>•</sup> and superoxide production.

Several studies have reported that PARP was implicated in NO<sup>•</sup> cytotoxicity (26, 27). Mebmer et al. (28) reported that NO<sup>•</sup> increases the intracellular caspase-3 by elevated expression or activation and mediates PARP cleavage. Proteolysis results in the split of its DNA binding vs. poly(ADP-ribose) polymerase activities. Moreover, PARP cleavage could result in endonuclease activation. In the present work, we confirmed that DNA damage induced by UVA/L-Arg treatment was relevant to PARP. Indeed, the addition of ABA, a potent inhibitor of PARP, prevented completely the formation of DNA lesions. In addition, ABA also reduced the amount of DNA damage in L-Arg-treated cells. It is believed that DNA damage elicits a rapid stress response in mammalian cells, which involves attachment of PARP to the strand breaks and extensive synthesis of short-lived polymers by the bound enzyme. Although PARP has no direct role in DNA excision repair, it binds tightly to DNA break and may interfere with repair if poly(ADP-ribose) synthesis is prevented (29). However, with massive PARP activation after extensive DNA damage, the ADP-ribose donor NAD<sup>+</sup> is depleted and subsequent ATP deprivation may represent a signal leading to cell death (30, 31). In UVA/L-Arg-treated cells, the PARP inhibitor ABA

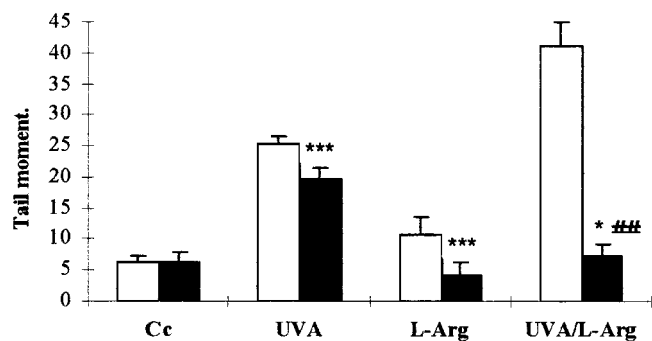


Figure 2. : DNA damage induced by UVA irradiation, L-Arg treatment, or both in HaCaT cells incubated or not with ABA. Yield of damage is represented by the mean tail moment of 50 cells per slide ( $n=3$ ). \*\*\* $P < 0.05$  UVA+ABA vs. UVA, UVA/L-Arg vs. L-Arg; \* $P < 0.001$  UVA/L-Arg+ABA vs. UVA/L-Arg; ## $P < 0.01$  UVA+ABA vs. UVA/L-Arg+ABA. Filled bars: with ABA; white bars: without ABA.



provided a protection against cell killing (percent of cell viability: 56.63 in ABA pretreated cells vs. 15.2 in untreated cells). Our observations suggest that PARP inhibition might maintain DNA integrity and protects cells against cell death. It may be one of the mechanisms by which pharmacological inhibition of PARP during oxidative stress exerts beneficial effects as it improves survival and prevents the degree of peroxynitrite-induced endothelial and epithelial dysfunction (32).

To better understand the cytotoxic effect of the combined treatment, UVA/L-Arg, we measured the antioxidant metalloenzymes activities. L-Arg treatment inactivated strongly intracellular GSH-Px. It was shown that GSH-Px was also inactivated by SNAP, which led to an exogenous NO generation (19). GSH-Px are antioxidative enzymes that metabolize various peroxides. The level of GSH-Px is higher than that of catalase in most cells. The  $K_m$  value of catalase for  $H_2O_2$  is higher than that of GSH-Px, suggesting the primary importance of GSH-Px in cells. Hence, the destruction of the balance between oxidants and antioxidants by reactive nitrogen species such as  $NO^\bullet$  and peroxynitrite through inhibition of GSH-Px could easily affect cellular homeostasis. In our models, we observed both GSH-Px and catalase inactivations. As UVA also inactivated the latter enzymes, the combined treatment strongly affected the antioxidant cell defenses. The inactivation of GSH-Px observed in the UVA/L-Arg model could be induced by direct binding of  $NO^\bullet$  to the amino acid residue (selenocysteine), at the catalytic center of the molecule (19). Because redox regulation of cells and GSH-Px activity are closely tied to apoptosis, inactivation of GSH-Px by  $NO^\bullet$  may be one cause of cell death. Immunoprecipitation and amino acid sequencing techniques identified manganese superoxide dismutase, the major antioxidant enzyme in mitochondria, as one of the targets of tyrosine nitration. *In vitro* studies demonstrated that peroxynitrite readily nitrates tyrosine residue of MnSOD and inhibits its enzymatic activity (33). In UVA/L-Arg-treated keratinocytes, no significant alteration of MnSOD was observed. However, we showed that MnSOD activity increases in irradiated cells so it could compensate a tyrosine nitration. SNAP decomposition in the culture medium also induced a significant increase of MnSOD in HaCaT cells.

We have demonstrated that UVA-irradiated keratinocytes HaCaT are able to generate  $NO^\bullet$  in the presence of the substrate of the NOS. The findings obtained using NOS inhibitor and SOD suggested that  $ONOO^-$  formation in the UVA/L-Arg-treated cells induced both DNA damage and cell death. The extent to which  $ONOO^-$  caused inactivation of metalloenzymes and DNA damage suggested that it

may be a causative factor of UVA-induced skin damage. The L-Arg/ $NO^\bullet$  pathway could be the foundation for the development of new approaches to the management and treatment of skin diseases. [F]

We thank Prof. A. Favier for stimulating discussions. We are grateful to C. Garrell for nitrite determination.

## REFERENCES

1. Moncada, S., and Higgs, A. (1993) Mechanisms of disease. *N. Engl. J. Med.* **329**, 2002–2012
2. Kim, Y.-M., De Vera, M. E., Watkins, S. C., and Billiar T. R. (1997) Nitric oxide protect cultured rat hepatocytes from tumor necrosis factor- $\alpha$ -induced apoptosis by inducing heat shock protein 70 expression. *J. Biol. Chem.* **272**, 1402–1411
3. Ioannidis, I., Batz, M., Paul, T., Korth, H.-G., Sustmann, R., and Groot H. (1996) Enhanced release of nitric oxide causes increased cytotoxicity of S-nitroso-N-acetyl-DL-penicillamine and sodium nitroprusside under hypoxic conditions. *Biochem. J.* **318**, 789–795
4. Bruch-Gerharz, D., Ruzicka, T., and Kolb-Bachofen, V. (1998) Nitric oxide in human skin: current status and future prospects. *J. Invest. Dermatol.* **110**, 1–7
5. Baudouin, J. E., and Tachon, P. (1996) Constitutive nitric oxide synthase is present in normal human keratinocyte. *J. Invest. Dermatol.* **106**, 428–431
6. Villiotou, V., and Deliconstantinos, G. (1995) Nitric oxide, peroxynitrite and nitroso-compounds formation by ultraviolet A (UVA) -irradiated human squamous cell carcinoma: potential role of nitric oxide in cancer prognosis. *Anticancer Res.* **15**, 931–942
7. Wang, R., Ghahary, A., Shen, Y. J., Scott, P. G., and Tredget, E. E. (1996) Human dermal fibroblasts nitric oxide and express both constitutive and inducible nitric oxide synthase isoforms. *J. Invest. Dermatol.* **106**, 419–427
8. Beckman, J. S., Beckman, T. W., Chen, J., Marshall, P. A., and Freeman, B. A. (1990) Apparent hydroxyl radical production by peroxynitrite: implications for endothelial injury from nitric oxide and superoxide. *Proc. Natl. Acad. Sci. USA* **87**, 1620–1624
9. Ischiropoulos, H., Zhu, L., and Beckman, J. S. (1992) Peroxynitrite formation from macrophage-derived nitric oxide. *Arch. Biochem. Biophys.* **298**, 446, 451
10. Van Der Vliet, A., Eiserich, J. P., Halliwell, B., and Cross, C. E. (1997) Formation of reactive nitrogen species during peroxidase-catalyzed oxidation of nitrite. *J. Biol. Chem.* **272**, 7617–7625
11. Eiserich, J. P., Hristova, M., Cross, C. E., Jones, A. D., Freeman, B. A., Halliwell, B., and van der Vliet A. (1998) Formation of nitric oxide-derived inflammatory oxidants by myeloperoxidase in neutrophils. *Nature (London)* **391**, 393–397
12. Boukamp, P., Petrussevska, R. T., Breitkreutz, D., Hornung, J., Markham, A., and Fusenig, N. E. (1988) Normal keratinization in a spontaneously immortalized aneuploid human keratinocyte cell line. *J. Cell Biol.* **106**, 761–771
13. Borenfreund, E., and Puerner, J. A. (1985) Toxicity determined *in vitro* by morphological alterations and neutral red absorption. *Toxicol. Lett.* **24**, 119–124
14. Singh, N. P., McCoy, M. T., Tice, R. R., and Schneider, E. L. (1988) A simple technique for the quantification of low levels of DNA damage in individual cells. *Exp. Cell Res.* **175**, 184–191
15. Emonet-Piccardi, N., Richard, M. J., Ravanat, J. L., Signorini, N., Cadet, J., and Béani, J. C. (1998) Protective effects of antioxidants against UVA-induced DNA damage in human skin fibroblasts in culture. *Free Rad. Res* **29**, 307–313
16. Leccia, M. T., Richard, M. J., Béani, J. C., Faure, H., Monjo, A. M., Cadet, J., Amblard, P., and Favier, A. (1993) Protective effect of selenium and zinc on UV-A damage on human skin fibroblasts. *Photochem. Photobiol.* **58**, 548–553
17. Beers, B., and Sizer, W. (1952) A spectrophotometric method for measuring the breakdown of hydrogen peroxide by catalase. *J. Biol. Chem.* **195**, 133–139
18. Parat, M. O., Richard, M. J., Leccia, M. T., Amblard, P., Favier, A., and Béani, J. C. (1995) Does manganese protect cultured

- human skin fibroblasts against oxidative injury by UVA, dithranol, and hydrogen peroxide? *Free Rad. Res.* **23**, 339–351
19. Asahi, M., Fujii, J., Suzuki, K., Seo, H. G., Kuzuya, T., Hori, M., Tada, M., Fujii, S., and Taniguchi, N. (1995) Inactivation of glutathione peroxidase by nitric oxide. *J. Biol. Chem.* **36**, 21035–21039
  20. Kim, Y.-M., Bergonia, H. A., Müller, C., Watkins, W. D., and Lancaster, J. R. (1995) Nitric oxide and intracellular heme. *Adv. Pharmacol.* **34**, 277–291
  21. Kim, Y.-M., Bergonia, H. A., Muller, C. Pitt, B. R., Watkins, W. D., and Lancaster, J. R. (1995) Loss and degradation of enzyme-bound heme induced by cellular nitric oxide synthesis. *J. Biol. Chem.* **270**, 5710–5713
  22. Filep, J. G., Lapiere, C., Lachance, S., and Chan, J. S. D. (1997) Nitric oxide co-operates with hydrogen peroxide in inducing DNA fragmentation and cell lysis in murine lymphoma cells. *Biochem. J.* **321**, 897–901
  23. Brüne, B., Götz, C., Mebmer, U., Sandau, K., Hirvonen, M.-R., and Lapetina, E. G. (1997) Superoxide formation and macrophage resistance to nitric oxide-mediated apoptosis. *J. Biol. Chem.* **272**, 7253–7258
  24. Wink, D. A., Hanbauer, I., Krishna, M. C., DeGraff, W., Gamson, J., and Mitchell, J. B. (1993) Nitric oxide protects against cellular damage and cytotoxicity from reactive oxygen species. *Proc. Natl. Acad. Sci. USA* **90**, 9813–9817
  25. Gutierrez, H. H., Nieves, B., Chumley, P., Rivera, A., and Freeman, B. A. (1996) Nitric oxide regulation of superoxide-dependent lung injury: oxidant-protective actions of endogenously produced and exogenously administered nitric oxide. *Free Rad. Biol. Med.* **21**, 43–52
  26. Rubbo, H., Radi, R., Trujillo, M., Telleri, R., Kalyanaraman, B., Barnes, S., Kirk, M., and Freeman, B. A. (1994) Nitric oxide regulation of superoxide and peroxynitrite-dependent lipid peroxidation. *J. Biol. Chem.* **269**, 26066–26075
  27. Radons, J., Heller, B., Burkle, A., Hartmann, B., Rodriguez, M.-L., Kroncke, V., and Kolb, H. (1994) Nitric oxide toxicity in islet cells involves poly(ADP-ribose) polymerase activation and concomitant NAD<sup>+</sup> depletion. *Biochem. Biophys. Res. Commun.* **3**, 1270–1277
  28. Mebmer, U. K., Reimer, D. M., Reed, J. C., and Brüne, B. (1996) Nitric oxide induced poly(ADP-ribose) polymerase cleavage in RAW 264.7 macrophage is blocked by Bcl-2. *FEBS Lett.* **384**, 162–166
  29. Inada, C., Yamada, K., Takane, N., and Nonaka, K. (1995) Poly(ADP-ribose) synthesis induced by nitric oxide in a mouse  $\beta$ -cell line. *Life Sci.* **56**, 1467–1474
  30. Virag, L., Scott, G. S., Cuzzocrea, S., Marmer, D., Salzman, A. L., and Szabo, C. (1998) Peroxynitrite-induced thymocyte apoptosis: the role of caspases and poly(ADP-ribose) synthetase (PARS) activation. *Immunology* **94**, 345–355
  31. Rosenthal, D. S., Ding, R., Simbulan-Rosenthal, C. M. G., Vaillancourt, J. P., Nicholson, D. W., and Smulson, M. (1997) Intact cell evidence for the early synthesis, and subsequent late apopain-mediated suppression, of poly(ADP-ribose) during apoptosis. *Exp. Cell Res.* **232**, 313–321
  32. Cuzzocrea, S., Zingarelli, B., and Constantino, G. (1997) Beneficial effects of 3-aminobenzamide, an inhibitor of poly(ADP-ribose) synthetase in a rat model of splanchnic artery occlusion and reperfusion. *Br. J. Pharmacol.* **121**, 1065–1074
  33. Mac Millan-Crow, L. A., Crow, J. P., Kerby, J. D., Beckman, J. S., and Thompson, J. A. (1996) Nitration and inactivation of manganese superoxide dismutase in chronic rejection of human renal allografts. *Proc. Natl. Acad. Sci. USA* **93**, 11853–11858

Received for publication November 20, 1998.

Revised for publication April 29, 1999.